C.P. No. 885

C.P. No. 885

MINISTRY OF AVIATION

AERONAUTICAL RESEARCH COUNCIL

CURRENT PAPERS

A Velocity Defect Relationship for the Outer Part of Equilibrium and Near Equilibrium Turbulent Boundary Layers

By

J. McQuaid

LONDON: HER MAJESTY'S STATIONERY OFFICE

1966

SIX SHILLINGS NET

C.P. No. 885

October, 1965

A Velocity Defect Relationship for the Outer Part of Equilibrium and near-Equilibrium Turbulent Boundary Layers

by

J. McQuaid

Engineering Department, Cambridge University

Summary

It is shown that the outer part of the velocity defect profiles for equilibrium turbulent boundary layers on solid surfaces can be satisfactorily reduced to an almost universal curve by the use of the velocity scale $U_* = U_1(d\Theta/dx)^{\frac{1}{2}}$, with $d\Theta/dx$ obtained from the momentum integral equation. The procedure thus uses a single scale for the complete range of the pressure gradient parameter π, whereas previously the use of U_τ as in Clauser's formulation is restricted to cases of finite wall shear stress, with an additional scale, as, for example, Mellor and Gibson's 'pressure' velocity U_p, being necessary to treat the zero wall stress layer. The present scale reduces to U_τ as required for the constant pressure layer and is simply related to U_p for the zero wall stress layer. The scale is also found to account well for the outer part of near-equilibrium layers, in particular for the constant pressure layer with uniformly distributed injection. Finally, by combining the relationship with the two-parameter family of mean velocity profiles of Thompson, a simple method is obtained for calculating the variation of the shape-parameter, H.

Replaces A.R.C.27 287.

1. Introduction

The problem of treating the mean velocity distribution in the outer part of turbulent boundary layers has occupied a number of workers in the past. The various approaches can be identified as belonging to one of the following two classes: i) The correlation of the departure of the velocity profile in the outer region from the law of the wall. The main contributions have been the law of the wake of Coles (1956) and the intermittency hypothesis of Sarnecki (1959), which has been used by Thompson (1965 A). ii) The correlation of the velocity defect in the layer as a function of y/δ and some appropriate pressure gradient parameter. The principal approaches have been the constant eddy viscosity analyses of Clauser (1956), Townsend (1956), Mellor and Gibson (1963) and Libby, Baronti and Napolitano (1964), and more recently the extended overlap analysis of Stevenson (1965 B). All of the constant eddy viscosity analyses are for the particular case of equilibrium layers.

This paper will be concerned with pointing out an interesting, but hitherto unobserved, regularity in the velocity defect in the outer part of the layer. Although the results can be expected to hold precisely only for equilibrium conditions, good agreement is shown with experiment for some near-equilibrium layers of practical interest.

2. Velocity Defect Relationship for the Outer Part of Equilibrium Layers

For constant pressure layers without transpiration, the velocity defect law of von Karman using U_τ as the velocity scale, viz.,

$$\frac{u - U_1}{U_\tau} = g(y/\delta) \ , \tag{1}$$

is well established for both smooth and rough walls (Clauser, 1954, 1956). The law holds throughout the layer except in the sublayer and blending region immediately adjacent to the wall. The constant pressure layer is a particular case of an equilibrium layer, that is a layer which has a constant upstream history and is thus governed by local conditions only. This condition is satisfied because the rate of change of the wall shear, the only force acting on the layer, with x is in practice very small and the local value of wall shear stress will be much the same as the value obtained by taking a mean over several boundary layer thicknesses upstream. For exact equilibrium, the wall shear stress must be constant, and Rotta (1962) has shown that this condition will be satisfied if the surface roughness distribution is such that the roughness scale varies directly with the distance from the leading edge. If the wall stress is changing rapidly, then the local value may differ considerably from such an integrated value and the velocity profiles will not follow equation (1). This has been shown by Clauser (1956) who used a corrugated roughness strip to produce rapid changes in wall stress.

For non-zero pressure gradients, the problem of defining the conditions for constant upstream history has been treated by Rotta (1955) and Clauser (1954). Clauser recognised that the velocity profiles in such layers should form a one-parameter family analogous to the Falkner-Skan family for laminar equilibrium profiles. Since constant pressure profiles must form a single member of such a family, and since the scheme of equation (1) is the only one which satisfactorily reduces them to a nearly universal curve, he concluded that the one-parameter family for turbulent equilibrium profiles would only be obtained when the profiles are plotted in the co-ordinates of equation (1), so that

$$\frac{u - U_1}{U_\tau} = g(y/\delta, \pi), \tag{2}$$

where π is an appropriate pressure gradient parameter which will be constant for any particular equilibrium layer. He managed to obtain experimentally two equilibrium layers and showed that the constant parameter is $\pi = \frac{\delta^*}{\tau_0}\frac{dp}{dx}$. The members of the family obtained by Clauser are reproduced in Fig. 1, where mean lines have been taken from his original figures.

The equilibrium layer obtained by Stratford (1959) for zero wall shear stress, introduces a difficulty into the formulation proposed by Clauser, since the profiles cannot now be plotted in the form of equation (2). To overcome this, Mellor and Gibson (1963) have used a 'pressure velocity' for cases where the influence of the pressure gradient dominates. They define

$$U_p^2 = \frac{\delta^*}{\rho}\frac{dp}{dx}, \tag{3}$$

and find that the use of U_p as velocity scale accounts for Stratford's profiles, as U_τ does for Clauser's. This procedure is somewhat unsatisfactory since it introduces the need for two velocity scales to cover the complete range of the pressure gradient parameter, π. A single velocity scale which equals U_τ for the constant pressure case and which can also be used with layers of the Stratford type is needed. Such a scale can be obtained from a consideration of the two-dimensional momentum integral equation, which, for constant pressure, can be written as

$$U_\tau^2 = U_1^2 \frac{d\theta}{dx}. \tag{4}$$

The use of $U_1(d\theta/dx)^{\frac{1}{2}}$ (with appropriate $d\theta/dx$) thus provides a single scale which can be used in all conditions and which reduces to U_τ as required for constant pressure. For layers with pressure gradient and transpiration, the scale follows as

$$U_1^{\,2}\,\frac{d\theta}{dx} = U_*^{\,2}\;,$$

$$= -(H + 2)\theta U_1\,\frac{dU_1}{dx} \pm V_oU_1 + \frac{\tau_o}{\rho}\;,$$

$$= (1 + \tfrac{2}{H})\,\frac{\delta^*}{\rho}\,\frac{dp}{dx} \pm V_oU_1 + U_\tau^{\,2}\;. \qquad (5)$$

($+ V_oU_1$ for injection, $-V_oU_1$ for suction).

The relationship between the two velocity scales is obtained as,

$$\frac{U_*^{\,2}}{U_\tau^{\,2}} = \Phi = (1 + \tfrac{2}{H})\pi \pm \frac{V_oU_1}{U_\tau^{\,2}} + 1. \qquad (6)$$

For any particular equilibrium layer, the shape parameter, H, will be nearly constant and hence the parameter Φ defined by equation (6) will be substantially a constant, since small variations in H have a minor effect. Φ could thus be used as an alternative to π for labelling members of the one-parameter family obtained on a solid surface. The value of Φ ranges from 0 for the flat plate asymptotic layer with suction to ∞ for separation. For the constant pressure case, $\Phi = 1$.

For a Stratford-type layer with $U_\tau = 0$, equation (5) becomes

$$U_*^{\,2} = (1 + \tfrac{2}{H})\,\frac{\delta^*}{\rho}\,\frac{dp}{dx}\;,$$

$$= (1 + \tfrac{2}{H})U_p^{\,2}\;.$$

U_* is thus a simple multiple of Mellor and Gibson's pressure velocity if H is again considered constant for an equilibrium layer.

The velocity defect profiles of Fig. 1 may now be transformed from $(u - U_1)/U_\tau$ to $(u - U_1)/U_*$ co-ordinates, using equation (6). This has been done using mean values of H, and values of π obtained by Mellor and Gibson from a re-examination of Clauser's data. The values of the parameters are shown in Table 1.

	H	π	U_τ/U_*
Pressure Distribution I	1.5	1.8	.439
Pressure Distribution II	1.8	8.0	.237

Table 1. Parameters of Clauser's Equilibrium Layers.

The transformed profiles are shown in Fig. 2, where it is seen that the procedure brings the profiles into close agreement with the constant pressure curve. Over the outer 60-70 per cent of the layer the agreement is within the scatter usually associated with the constant pressure curve. The curves do, however, diverge in the inner part; this is to be expected, since the inner region is known to be relatively insensitive to pressure gradient and a velocity scale such as U_*, which can depend significantly on the pressure gradient, cannot thus be a realistic velocity scale. The problem of treating the inner part will be discussed later.

Clauser has plotted his results in terms of δ, the value of y at which $u/U_1 = 1.0$, which in practice is difficult to determine with precision. In the profile comparisons to follow, the more well-defined thickness, $\bar{\delta}$, at which $u/U_1 = .995$, will be used.* The equilibrium profiles of Stratford (1959) for $\pi = \infty$ and of Bradshaw and Ferriss (1965) for $\pi = 5.4$ are shown plotted in the universal co-ordinates in Figs. 4 and 5. It is seen that for both of these cases the data again fall close to the constant pressure curves.

It can thus be reasonably concluded that the outer part of equilibrium velocity profiles is well represented by the universal relationship

$$\frac{u - U_1}{U_*} = g(\frac{y}{\bar{\delta}}). \qquad (7)$$

---

* To obtain the likely spread of the constant pressure velocity defect plot in these co-ordinates, use is made of the recently formulated two parameter family of mean velocity profiles of Thompson (1965 A) together with suitable values of H and R_θ. Accepting $H = 1.37$, $R_\theta = 3.2 \times 10^3$ and $H = 1.26$, $R_\theta = 5 \times 10^4$ as reasonable extremes, the corresponding profiles have been extracted from the family. The skin friction coefficients have been obtained from Thompson's skin friction law. The velocity defect profiles thus obtained should well represent the spread of constant pressure results. They are shown on all the profile comparisons, the lower curve being that at the higher Reynolds number. In Fig. 3, they are plotted in the y/δ form for comparison with the mean curve used by Clauser.

For the inner part, an overlap analysis similar to that of Millikan (1938) may be invoked to obtain the form of equation (7) in this region. The law of the wall is assumed to be

$$\frac{u}{U_\tau} = f\left(\frac{U_\tau y}{\nu}\right) . \qquad (8)$$

Any effects of pressure gradients on the law of the wall are thus neglected for the purposes of the present analysis. This assumption is supported for a wide range of pressure gradients by the experiments of Ludwieg and Tillmann (1950).

The velocity defect law is

$$\frac{u - U_1}{U_*} = g\left(\frac{y}{\delta} , \pi\right) . \qquad (9)$$

(The function g depends only on y/δ in the outer part; it has been noted that different equilibrium layers (i.e. different values of π) result in different forms for g in the inner part and hence a dependence on π is here included).

If a region of overlapping between equations (8) and (9) is assumed, then

$$\frac{u}{U_\tau} = f\left(\frac{U_\tau y}{\nu}\right) = \frac{U_*}{U_\tau}\, g\left(\frac{y}{\delta} , \pi\right) + \frac{U_1}{U_\tau} .$$

Now,

$$\frac{df}{d\left(\frac{U_\tau y}{\nu}\right)} = \frac{1}{\frac{U_\tau \delta}{\nu}} \cdot \frac{\partial f}{\partial\left(\frac{y}{\delta}\right)} ,$$

$$= \frac{1}{\frac{U_\tau \delta}{\nu}} \cdot \frac{U_*}{U_\tau} \cdot \frac{\partial g}{\partial\left(\frac{y}{\delta}\right)} ,$$

or
$$\frac{U_\tau y}{\nu}\, f'\left(\frac{U_\tau y}{\nu}\right) = \frac{U_*}{U_\tau} \cdot \frac{y}{\delta} \cdot g'\left(\frac{y}{\delta} , \pi\right) , \qquad (10)$$

where the primes denote differentiation with respect to $\frac{U_\tau y}{\nu}$ or $\frac{y}{\delta}$ as appropriate.

The ratio U_*/U_τ would in general be expected to depend on both π and U_τ/U_1 but it is seen from equation (6) that this latter dependence only enters through the dependence of H on on U_τ/U_1 which the experiments of Clauser have shown to be very weak. Hence it is assumed that this dependence can be neglected and so

$$\frac{U_*}{U_\tau} = h(\pi) \quad \text{only.}$$

Hence equation (10) becomes

$$\frac{U_\tau y}{\nu} \cdot f'\left(\frac{U_\tau y}{\nu}\right) = h(\pi) \cdot \frac{y}{\delta} \cdot g'\left(\frac{y}{\delta}, \pi\right) ,$$

$$= 1/\kappa ,$$

where κ is a constant independent of $\frac{U_\tau y}{\nu}$, $\frac{y}{\delta}$ and π and thus has the same value as for constant pressure.

Hence $$\frac{u}{U_\tau} = \frac{1}{\kappa} \log_e \frac{U_\tau y}{\nu} + B ,$$

where B is independent of π, and,

$$\frac{u - U_1}{U_*} \cdot h(\pi) = \frac{1}{\kappa} \log_e \frac{y}{\delta} + C ,$$

or $$\frac{u - U_1}{U_\tau} = \frac{1}{\kappa} \log_e \frac{y}{\delta} + C , \tag{11}$$

where C is a function of π. Equation (11) agrees with the observation of Clauser (1954) that a logarithmic plot of $(u - U_1)/U_\tau$ in the overlap region has the same slope as the constant pressure profile but an intercept which depends on the equilibrium parameter π.

3. Boundary Layers with Uniformly Distributed Suction or Injection

While the use of a single local parameter such as U_* as the scale velocity for the outer region can only be strictly justified for equilibrium conditions, in practice there are a number of types of layer where the departure from equilibrium is usually not very great. A particular case of such layers is the constant pressure layer with uniformly distributed suction or injection, for which a number of experimental results are available. For this case, equation (5) becomes

$$U_*^2 = U_\tau^2 \pm V_0 U_1 , \tag{12}$$

and $$\Phi = 1 \pm \frac{V_0 U_1}{U_\tau^2} . \tag{13}$$

A comparison of this velocity scale with some other recently proposed scales for layers with injection will be given later.

For large injection rates, U_τ tends to zero and so equation (12) becomes

$$U_*^2 = V_0 U_1 \; . \qquad (14)$$

For the particular case of the flat plate asymptotic layer with suction, $d\theta/dx = 0$ and hence $U_* = 0$. This result accords with the experimentally verified fact that there is little or no 'outer part' to this type of layer and an inner region analysis holds practically to the outer edge.

Some results obtained by the author* for injection on a flat plate in zero pressure gradient are shown in Fig. 6. Data obtained in similar conditions by Mickley and Davis (1957) and on an axisymmetric body in zero pressure gradient by Stevenson (1965 A) are shown in Figs. 7 and 8. In all three cases the agreement with the defect curves for zero transpiration is good.

It is of interest to note that the constant pressure layer with uniformly distributed injection is not an exact equilibrium layer in the sense already discussed. To correspond with the required condition that U_τ/U_1 be constant for the flat plate zero transpiration layer, it would be expected that the more general exact equilibrium layer is obtained when U_*/U_1 is constant. The variation of U_τ/U_1 with x prevents U_*/U_1 from being constant, but just as for the smooth flat plate layer with zero transpiration, the rate of change of U_τ/U_1, and hence of U_*/U_1, with x is small and the layer is very nearly in equilibrium.** The constant pressure layer with uniform injection should, in fact, be closer to equilibrium than that with zero transpiration, since the effect of the variation of U_τ^2/U_1^2 in the expression for U_*^2/U_1^2 is suppressed by the constant V_0/U_1 term. It follows from equation (14) that the continuously separating layer obtained at the "blow-off" point*** analogous to the layer of Stratford on an impermeable surface, should be an exact equilibrium layer.

---

* These results and those of the author referred to later are being prepared for separate publication.

** E.g. from the author's results for $V_0/U_1 = .0033$, U_*^2/U_1^2 changes from .0042 at $R_\theta = 1200$ to .0036 at $R_\theta = 9{,}600$.

*** At about $V_0/U_1 = .011$, according to Hacker (1963).

From the comparisons presented in Figs. 6 to 8, it is clear that the departures of constant pressure, constant injection rate layers from equilibrium are insignificant and that the present relationship adequately represents the data in the outer part of the layer.

4. Boundary Layers with Arbitrary Pressure Distributions

Except in the region close to separation where $d\Theta/dx$ goes through a maximum,* it is generally the case that changes in $d\Theta/dx$ and hence in U_*/U_1 occur comparatively slowly. Boundary layers in the arbitrary pressure distributions encountered in practice can thus be considered to be in a state of near equilibrium, as has also been concluded by Nash (1965). Two layers with injection in arbitrary pressure distributions obtained by the author**, together with the layer of Newman (1951) on a solid surface have been analysed and the results are shown in Figs. 9, 10 and 11. The agreement with the constant pressure curves is reasonable; the departures can very adequately be explained if the distribution of local $d\Theta/dx$ is compared with that obtained from the profile in the following way. Equation (7) allows of a scheme for the outer region analogous to that of Clauser for the inner region using the law of the wall. Equation (7) is rearranged to give

$$\frac{u}{U_1} = 1 - \frac{U_*}{U_1}\, g\left(\frac{y}{\delta}\right),$$

$$= 1 - \left(\frac{d\Theta}{dx}\right)^{\frac{1}{2}} g\left(\frac{y}{\delta}\right). \qquad (15)$$

Using equation (15), a chart may be constructed with curves of constant $d\Theta/dx$ on which profiles may be plotted directly as u/U_1 versus y/δ and the value of $d\Theta/dx$ appropriate to the profile read off. The value of $d\Theta/dx$ so obtained will only be equal to the local value for equilibrium layers. However, it can be expected that the outer region of layers in arbitrary pressure distributions will adjust to some value of $d\Theta/dx$ representing the integrated effect of upstream influences. For layers in near equilibrium, where $d\Theta/dx$ will not be changing rapidly, this value will not be far removed from the local value. Such a chart can thus be used to determine how far a layer is removed from equilibrium.

---

* Throughout the remainder of the paper, $d\Theta/dx$ will be written as shorthand for the right-hand side of the two-dimensional momentum integral equation. It will thus not necessarily be the same as the experimental value of $d\Theta/dx$.

** For these layers, the injection rates and pressure gradient parameters are:

Pressure Distribution I: $V_o/U_1 \doteqdot .002$; $(H+2)\,\frac{\Theta}{U_1}\frac{dU_1}{dx} \doteqdot -.002$.

Pressure Distribution II: $V_o/U_1 \doteqdot .008$; $(H+2)\,\frac{\Theta}{U_1}\frac{dU_1}{dx} \doteqdot +.0035$.

Since, however, the constant pressure velocity defect curve for smooth wall data is not truly universal, but changes slowly with Reynolds number, there is some difficulty about drawing an acceptable "mean" curve through the data to represent the function g. For any of the particular layers which have been examined, the range of Reynolds number covered is small. In particular, for the author's data of Figs. 6, 9 and 10, the lower constant pressure curve seems to be a good "mean" curve. This same "mean" curve would not represent as well, for instance, the data of Bradshaw and Ferriss. In order to examine the departures from equilibrium in the layers of Figs. 9 and 10, this "mean" curve is used to construct the chart shown in Fig. 12, where some typical profiles are also shown. Since any "mean" curve used in the construction of the chart will not give curves of constant $d\Theta/dx$ which pass through the point $u/U_1 = .995$, $y/\delta = 1.0$, the "mean" curve is used for the range $y/\delta = .2$ to $.8$ and each curve is then faired into this point.

The appropriate value of $d\Theta/dx$ for each of the profiles in these layers has been obtained using the chart and is compared with the corresponding value from the momentum integral equation in Figs. 13a and 13b. It is seen that the maxima and minima in the distribution of $d\Theta/dx$ are reproduced in the profiles, with a lag due to the finite response of the outer part of the layer. The boundary layer thickness for both of these layers is about 1" so that in terms of boundary layer thickness the layer adjusts reasonably rapidly to perturbations in local conditions.

5. Comparisons of the Present Velocity Scale with some Previous Proposals for Layers with Suction or Injection

For the case of the constant pressure layer with uniform injection, a velocity defect law with a velocity scale, called U_τ^*, based on the maximum shear stress in the layer has been proposed by Mickley and Smith (1963) and Mickley, Smith and Fraser (1964, 1965). It is of interest to compare their proposal with that put forward here as equation (12). In their latest paper, they present a correlation of U_τ^*/U_τ against $\left(1 + \frac{V_o U_1}{U_\tau^2}\right)^{1/2}$ or, in this notation, against U_*/U_τ; this is reproduced here as Fig. 14. If the two velocity scales are to correlate the data for layers with injection, then $U_\tau^* = U_*$ and their correlation should be the straight line $U_\tau^*/U_\tau = U_*/U_\tau$ shown in Fig. 14. It is seen that there is a discrepancy between the two proposals which increases with the injection parameter. However, Mickley et al. point out that their procedure correlates the data of Fraser on to a curve with ordinates about 6% greater than the constant pressure, zero transpiration curve. From Fig. 14, it is seen that U_τ^*/U_τ is of the order of 6 to 10% smaller than U_*/U_τ for the data of Fraser, so that the use of U_*/U_τ would in fact bring their data into closer agreement with the zero transpiration curve, thus supporting the proposal made here. The author's results when analysed in this way behave similarly, the ordinates of the defect curves obtained using U_τ^* increasing with V_o/U_1 in general agreement with the trend of Fig. 14.

Stevenson (1963 A) has proposed a defect law

$$2\,\frac{U_\tau}{V_o}\cdot\left[\left(1+\frac{V_oU_1}{U_\tau^2}\right)^{\frac{1}{2}}-\left(1+\frac{V_ou}{U_\tau^2}\right)^{\frac{1}{2}}\right]=g\left(\frac{y}{\delta}\right) \tag{16}$$

which he has shown to be in good agreement with his own data and the lower injection rate data of Mickley and Davis. Equation (16) can be re-arranged to

$$\frac{U_1-u}{\frac{1}{2}\left[(U_\tau^2+V_oU_1)^{\frac{1}{2}}+(U_\tau^2+V_ou)^{\frac{1}{2}}\right]}=g\left(\frac{y}{\delta}\right).$$

For low to moderate values of V_o/U_1, the local velocity u in the outer part of the layer will be about $.8U_1$ or $.9U_1$ so that to a good approximation

$$\frac{1}{2}\left[(U_\tau^2+V_oU_1)^{\frac{1}{2}}+(U_\tau^2+V_ou)^{\frac{1}{2}}\right]=(U_\tau^2+V_oU_1)^{\frac{1}{2}}$$
$$=U_* .$$

Thus for low to moderate values of V_o/U_1, the defect law of Stevenson and that proposed here are very nearly the same. Only at high injection rates (above V_o/U_1 of about 0.006) will the difference become significant.

6. Prediction of Shape Factor H

The two-parameter profile family of Thompson (1965 A) gives

$$\frac{u}{U_1}=f_1\left(\frac{y}{\theta},\,H,\,R_\theta\right),$$

$$=f_1\left(\frac{y}{\delta}\cdot\frac{\delta}{\theta},H,\,R_\theta\right),$$

$$=f_1\left(\frac{y}{\delta},\,H,\,R_\theta\right),$$

since $\qquad \frac{\delta}{\theta}=f_2\,(H,\,R_\theta)\,.$

Hence $$\left(1 - \frac{u}{U_1}\right)_{\frac{y}{\delta} = \text{const.}} = f_3(H,\ R_\theta) \quad . \qquad (17)$$

The velocity defect relationship proposed here gives

$$\frac{U_1 - u}{U_*} = g\left(\frac{y}{\delta}\right) \text{ for } y/\delta \text{ greater than about } 0.3,$$

$$\text{or} \quad \left(1 - \frac{u}{U_1}\right)_{\frac{y}{\delta} = \text{const.}} = \text{const.} \frac{U_*}{U_1} ,$$

$$= \alpha \ \left(\frac{d\theta}{dx}\right)^{\frac{1}{2}} . \qquad (18)$$

The profile family gives the function f_3 in equation (17) while the constant α can be obtained at whatever value of y/δ is chosen. Equations (17) and (18) may be combined to give

$$\frac{d\theta}{dx} = f_4(H,\ R_\theta) \ ,$$

or, more usefully,

$$H = f_5(R_\theta,\ \frac{d\theta}{dx}) \ . \qquad (19)$$

Equation (19) is thus an auxiliary equation for the calculation of H development. It will be expected to hold strictly only for equilibrium layers on solid surfaces, the latter restriction being due to the profile family used. It should, however, give reasonable agreement for layers near equilibrium. For a case of particular practical interest, that of a layer in an adverse pressure gradient with $d\theta/dx$ increasing up to near separation, it will tend to give a predicted H development which will lead the experimental. In the region of separation, however, the prediction will fail, due to the rapid changes which occur in $d\theta/dx$.

The function f_5 in equation (19) has been determined from the profile family using a value of $y/\delta = 0.6$ and is shown in chart form in Fig. 15. For this value of y/δ, the value of α ranges from about 1.9 to 2.1.

Fig. 15 has been used together with both values of α to obtain H developments for several equilibrium and non-equilibrium layers. The results are shown in Figs. 16a to 16e. Also shown are the predictions of Head (1958) and Thompson, reproduced from Thompson (1965 B). For Clauser's first equilibrium layer and for the equilibrium part of Clauser's second layer*, the comparison for $\alpha = 2.1$ gives good agreement. For Bradshaw and Ferriss' equilibrium layer, the comparison for $\alpha = 1.9$ is in excellent agreement with experiment. It may be noted that these two values of α are within the spread of constant pressure boundary layer data. For the non-equilibrium layers of Schubauer and Klebanoff (1951) and of Newman (1951), the agreement can be considered satisfactory up to the region of separation, and compares reasonably with the predictions of Head and Thompson.

In all these comparisons, $d\theta/dx$ has been obtained from the two-dimensional momentum integral equation, using the measured values of H. They are therefore not predictions of H development in the usual sense, but serve as indicators of the general compatibility of the measured H and $d\theta/dx$ in the layers with the relation obtained from the defect law and shown in Fig. 15. In a proper calculation, the procedure would be to estimate a value of H at the station considered, use it with the known R_θ to obtain $d\theta/dx$ from the momentum integral equation; the value of H corresponding to these values of $d\theta/dx$ and R_θ could then be obtained from Fig. 15 and compared with the estimate. The procedure could be repeated until the estimated H and the value from the chart agree.

7. Acknowledgements

The author would like to thank his supervisor, Dr. L.C. Squire, for help and encouragement, and Drs. M.R. Head and B.G.J. Thompson for useful discussion during the course of this work. He also wishes to thank Dr. T.N. Stevenson for making available his experimental results and those authors whose data, made available to the Department of Engineering at Cambridge in the past, have been used in the present work.

8. Notation

B, C	coefficients in profile laws in overlap region
C_p	pressure coefficient used by Stratford $\left(= 1 - \frac{U_1^2}{U_o^2}\right)$
H	profile Shape Parameter $(= \delta^*/\theta)$
p	local static pressure
R_θ	boundary layer Reynolds number $(= U_1\theta/\nu)$
u	x-component of velocity in the boundary layer
U_1	free stream velocity
U_o	value of U_1 at reference station

---

* Between x = 152" and x = 230", according to Mellor and Gibson.

U_τ	wall shear velocity $(=(\tau_o/\rho)^{\frac{1}{2}})$
U_τ^*	velocity scale based on maximum shear stress used by Mickley et al.
U_*	velocity scale for outer region
U_p	pressure velocity used by Mellor and Gibson $\left(= \left(\frac{\delta^*}{\rho}\frac{dp}{dx}\right)^{\frac{1}{2}}\right)$
V_o	injection or suction velocity
x,y	localised rectangular Cartesian co-ordinates; x is measured along the surface in the longitudinal direction; y is measured normal to the surface
α	constant in relationship for velocity defect (equals $(U_1 - u)/U_*$ at $y/\bar{\delta} = 0.6$)
δ	value of y at $u/U_1 = 1$
$\bar{\delta}$	value of y at $u/U_1 = 0.995$
δ^*	displacement thickness $\left(= \int_0^\infty (1 - u/U_1)dy\right)$
θ	momentum loss thickness $\left(= \int_0^\infty \frac{u}{U_1}\left(1 - \frac{u}{U_1}\right) dy\right)$
π	equilibrium pressure gradient parameter $(= \frac{\delta^*}{\tau_o}\frac{dp}{dx})$
κ	universal constant in the mixing length relationship
Φ	parameter of family of equilibrium profiles
ν	kinematic viscosity
ρ	density
τ_o	wall shear stress.

9. References

Bradshaw, P. and Ferriss, D.H. 1965 The response of a retarded turbulent boundary layer to the sudden removal of pressure gradient. A.R.C.26 758.

Clauser, F.H. 1954 Turbulent boundary layers in adverse pressure gradients. J. Aero. Sci., Vol. 21, pp.91-108.

Clauser, F.H. 1956 The turbulent boundary layer. Adv. in Appl. Mech., Academic Press, New York, Vol. 4, pp.1-51.

Coles, D. 1956 The law of the wake in the turbulent boundary layer. J. Fluid Mech., Vol. 1, pp.191-226.

Hacker, D.S. 1963 Comment on 'Velocity defect law for a transpired turbulent boundary layer'. A.I.A.A. Journal, Vol. 1, pp.2676-2677.

Head, M.R. 1958 Entrainment in the turbulent boundary layer. A.R.C. R & M 3152.

Libby, P.A., Baronti, P.O. and Napolitano, L. 1964 Study of the incompressible turbulent boundary layer with pressure gradient. A.I.A.A. Journal, Vol. 2, pp.445-452.

Ludwieg, H. and Tillmann, W. 1950 Investigations of the wall shearing stress in turbulent boundary layers. N.A.C.A. TM 1285.

Mellor, G.L. and Gibson, D.M. 1963 Equilibrium turbulent boundary layers. Dept. of Aerospace and Mechanical Sciences, Princeton Univ., Rep. FLD No. 13.

Mickley, H.S. and Davis, R.S. 1957 Momentum transfer for flow over a flat plate with blowing. N.A.C.A. TN 4017.

Mickley, H.S. and Smith, K.A. 1963 Velocity defect law for a transpired turbulent boundary layer. A.I.A.A. Journal, Vol. 1, p.1685.

Mickley, H.S., Smith, K.A. and Fraser, M.D.	1964	Velocity defect law for a transpired turbulent boundary layer. A.I.A.A. Journal, Vol. 2, pp.173-174.
Mickley, H.S., Smith, K.A. and Fraser, M.D.	1965	Velocity defect laws for transpired turbulent boundary layers. A.I.A.A. Journal, Vol. 3, pp.787-788.
Millikan, C.B.	1938	A critical discussion of turbulent flows in channels and circular tubes. Proc. 5th Int. Congr. Appl. Mech., Cambridge, Mass., pp.386-392.
Nash, J.F.	1965	Turbulent boundary layer behaviour and the auxiliary equation. Nat. Phys. Lab. Aero Rep. No. 1137; A.R.C. C.P. No. 835.
Newman, B.G.	1951	Some contributions to the study of turbulent boundary layers near separation. Austr. Dept. Supply Rep. No. ACA-53.
Rotta, J.C.	1955	Similar solutions of turbulent boundary layers. J. Aero. Sci., Vol. 22, pp.215-216.
Rotta, J.C.	1962	Turbulent boundary layers in incompressible flow. Progress in Aero. Sci., Pergamon Press, Oxford, Vol. 2. pp.1-220.
Sarnecki, A.J.	1959	The turbulent boundary layer on a permeable surface. Ph.D. Dissertation, Univ. of Cambridge.
Schubauer, G.B. and Klebanoff, P.S.	1951	Investigation of separation of the turbulent boundary layer. N.A.C.A. Report 1030.
Stevenson, T.N.	1963 A	A modified velocity defect law for turbulent boundary layers with injection. A.R.C.25 797.

Stevenson, T.N. 1963 B A law of the wall for turbulent boundary layers with suction or injection. A.R.C.26 025.

Stevenson, T.N. 1965 A Experiments on injection into an incompressible turbulent boundary layer. A.R.C.26 989.

Stevenson, T.N. 1965 B The mean flow in the outer region of turbulent boundary layers. Proc. AGARD Symposium, Naples, AGARDograph 97, pp.281-314.

Stratford, B.S. 1959 An experimental flow with zero skin friction throughout its region of pressure rise. J. Fluid Mech., Vol. 5, pp.17-35.

Thompson, B.G.J. 1965 A A new two-parameter family of mean velocity profiles for incompressible turbulent boundary layers on smooth walls. A.R.C. R. & M. 3463.

Thompson, B.G.J. 1965 B The calculation of shape-factor development in incompressible turbulent boundary layers with or without transpiration. Proc. AGARD Symposium, Naples, AGARDograph 97, pp.159-190.

Townsend, A.A. 1956 The properties of equilibrium turbulent boundary layers. J. Fluid Mech., Vol. 1, pp.561-573.

D 61496/1/Dd.125875 K4 9/66 XL & CL

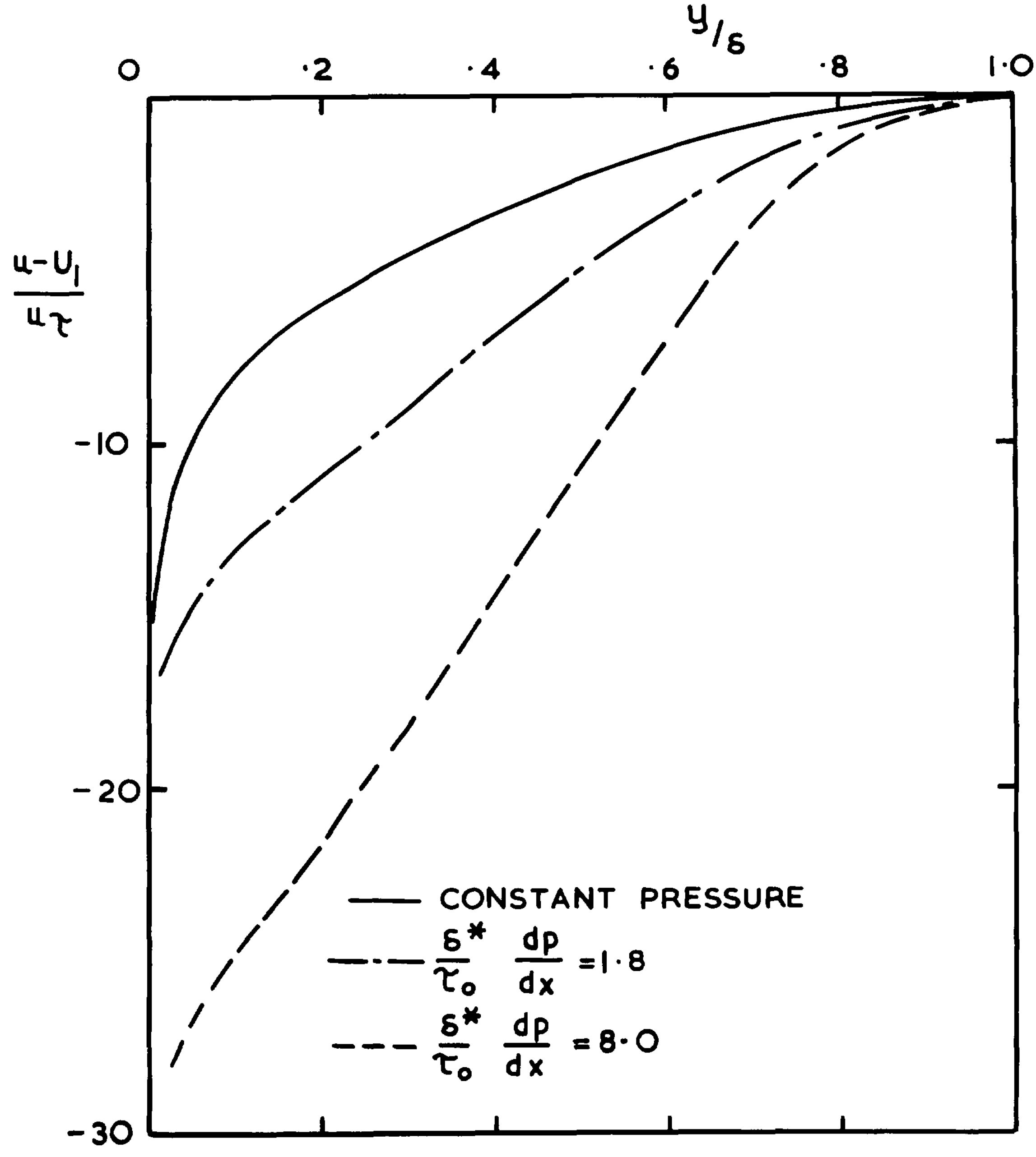

FIG. 1 EQUILIBRIUM PROFILES OF CLAUSER (1954)

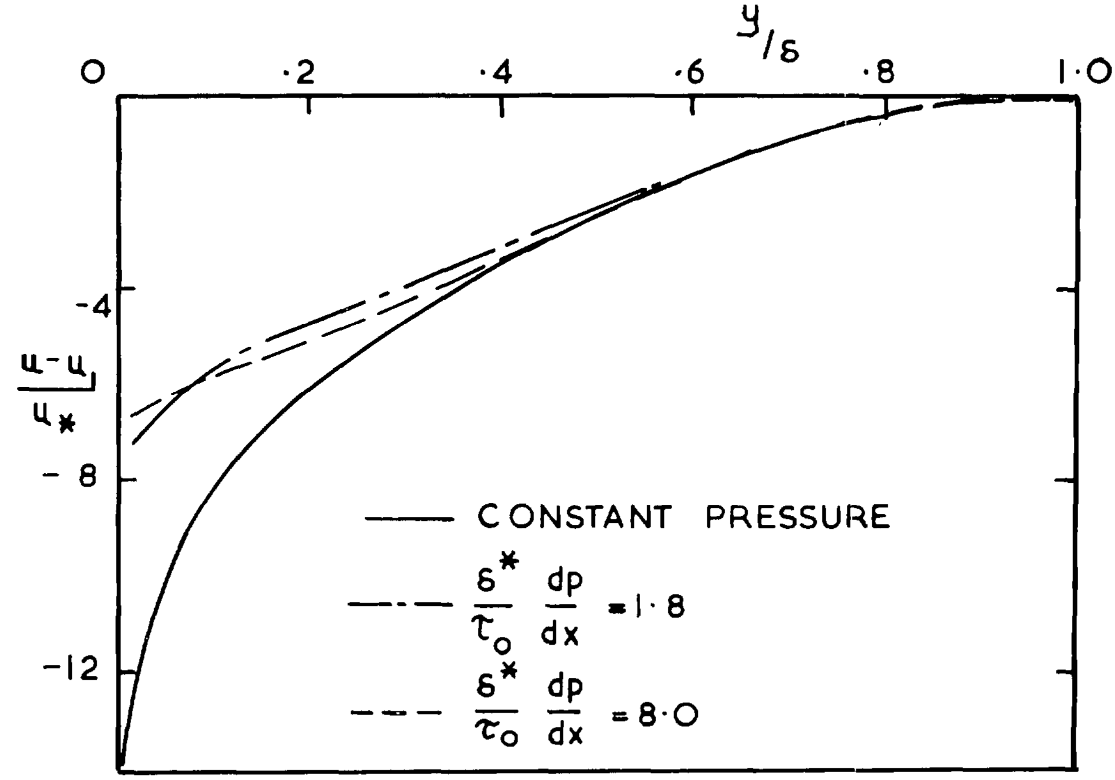

FIG. 2 TRANSFORMATION OF FIG. 1 FROM u_τ TO u_* AS VELOCITY SCALE

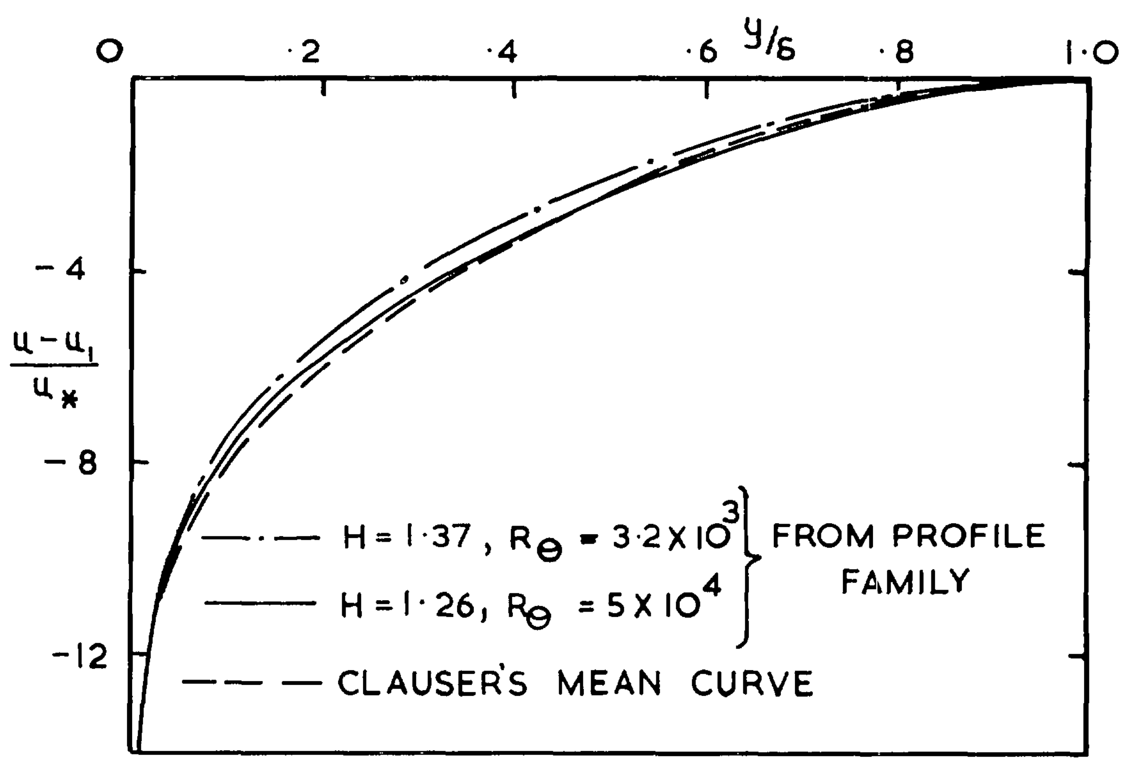

FIG. 3 COMPARISON OF VELOCITY DEFECT CURVES

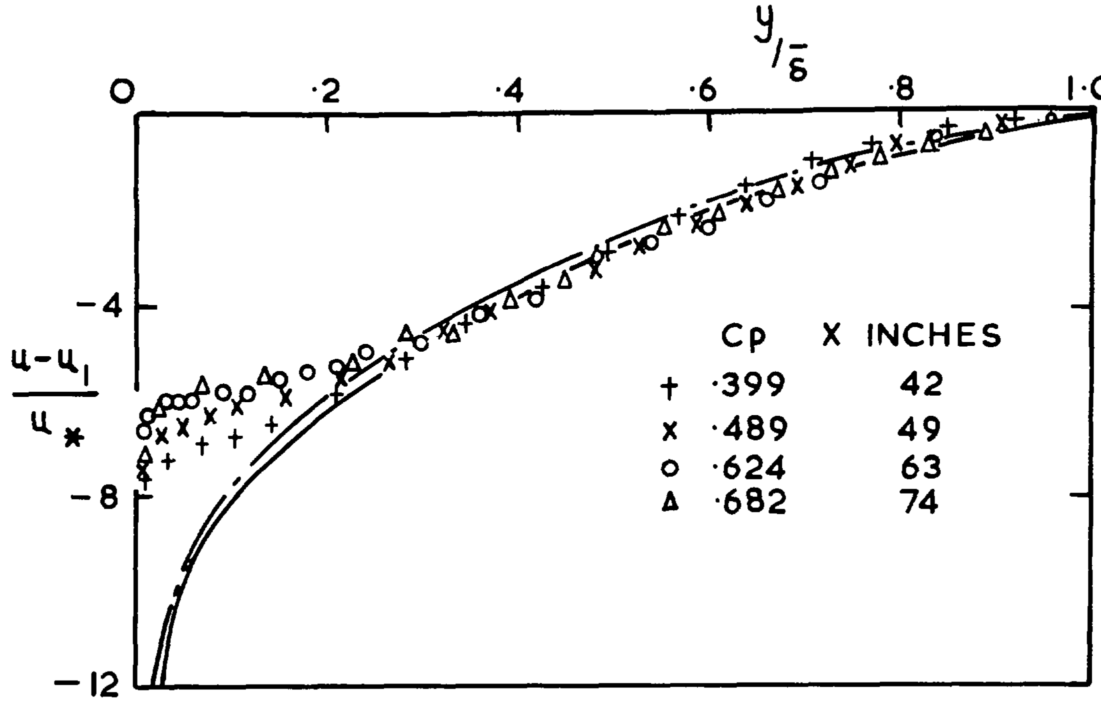

FIG. 4 STRATFORD (1959) EQUILIBRIUM LAYER WITH $\frac{\delta^*}{\tau_0}\frac{dp}{dx} = \infty$

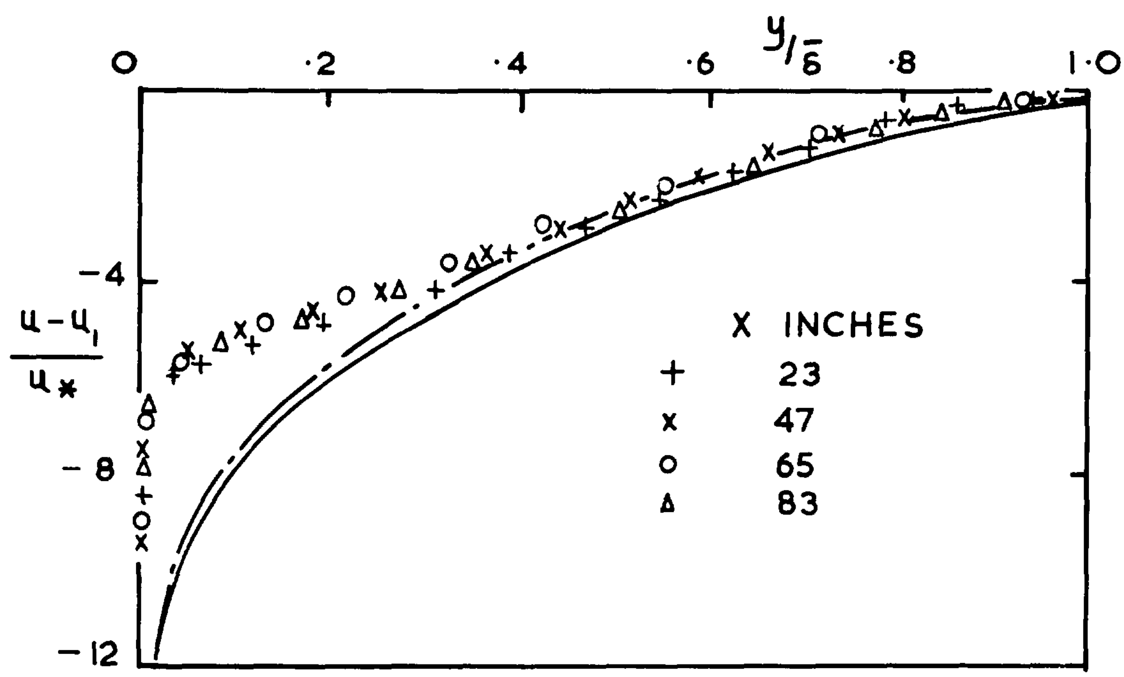

FIG. 5 BRADSHAW (1965) EQUILIBRIUM LAYER WITH $\frac{\delta^*}{\tau_0}\frac{dp}{dx} = 5{\cdot}4$

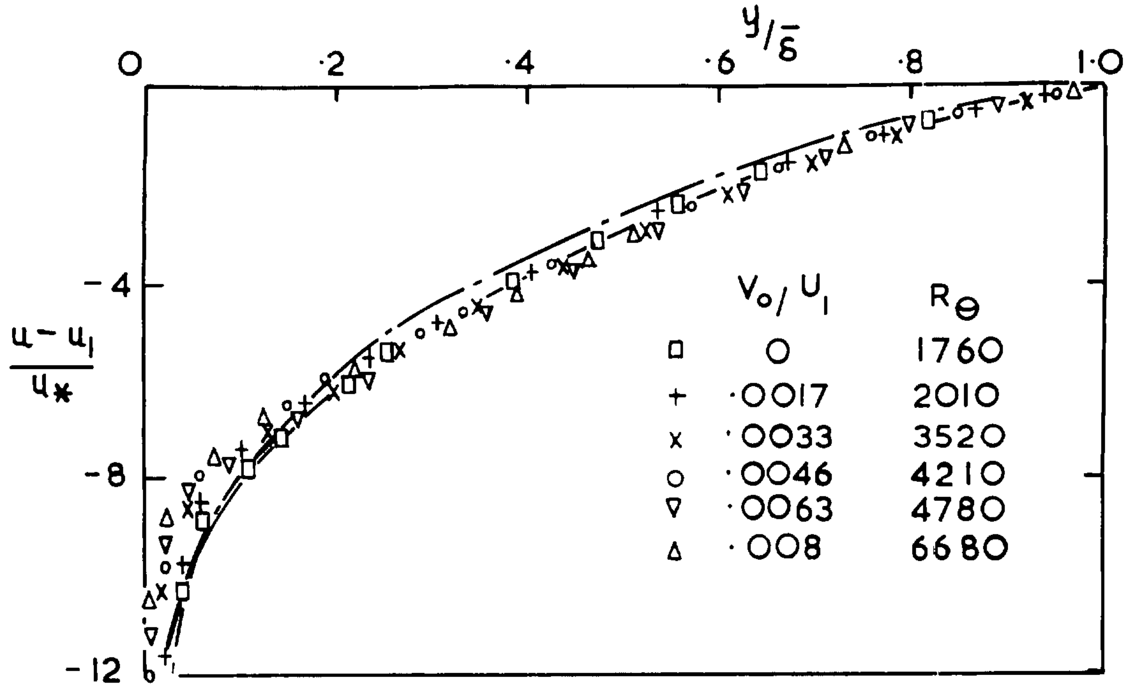

FIG. 6 DATA OF THE AUTHOR: INJECTION IN ZERO PRESSURE GRADIENT

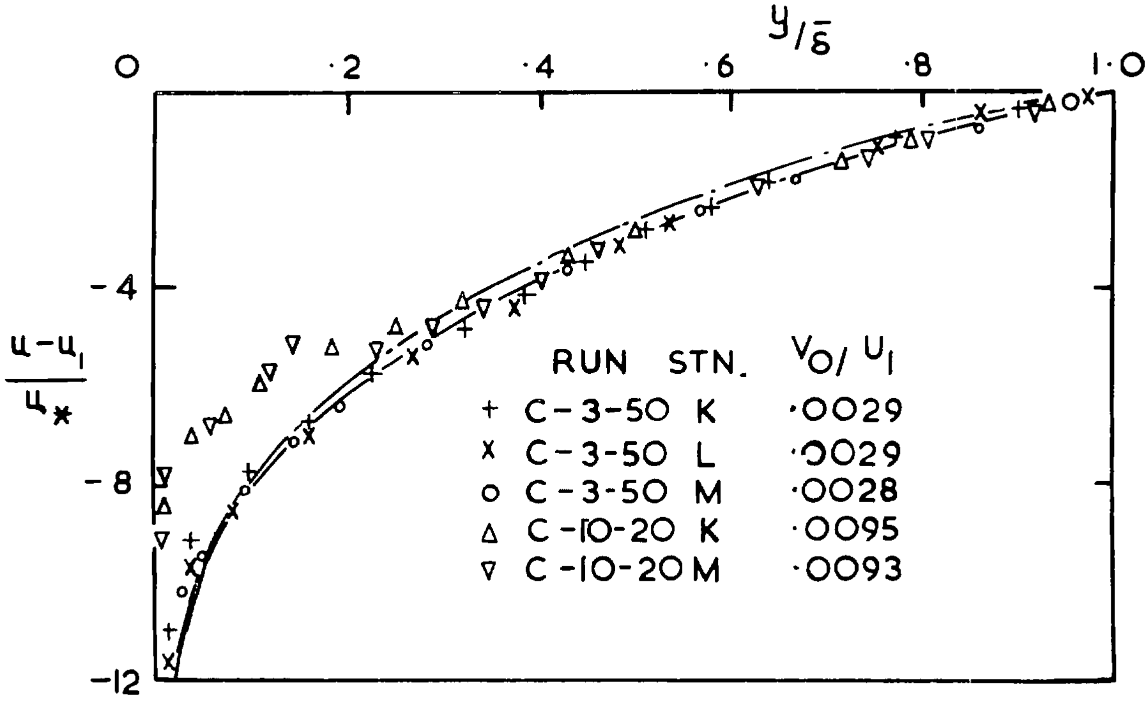

FIG. 7 MICKLEY & DAVIS (1957) INJECTION IN A SMALL FAVOURABLE PRESSURE GRADIENT

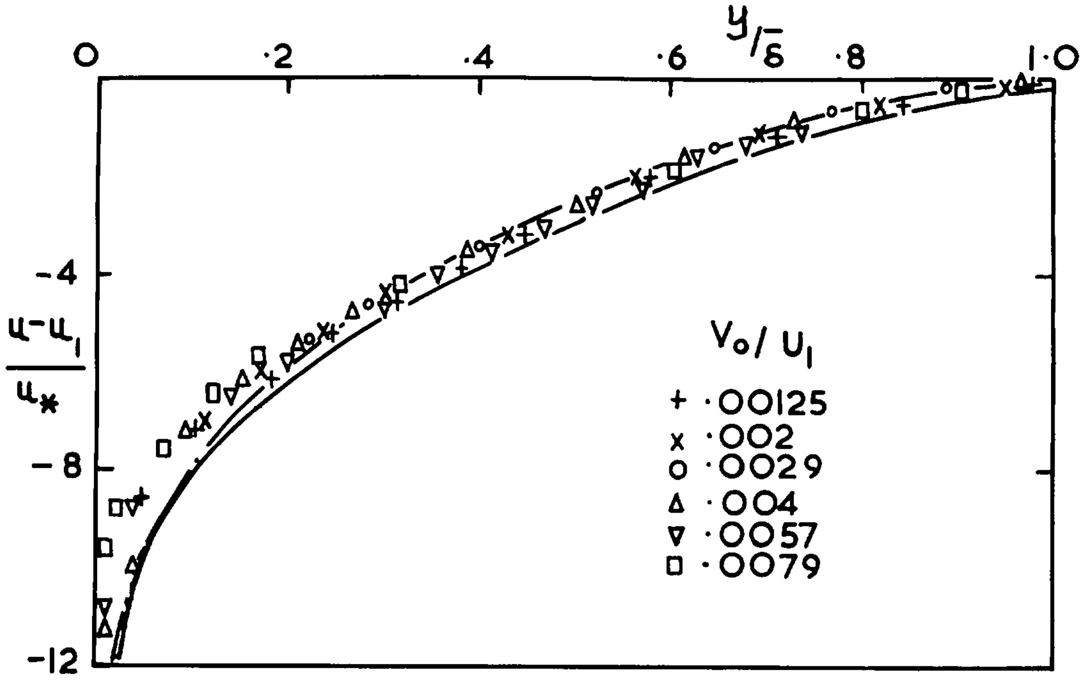

FIG. 8 STEVENSON (1965A) INJECTION IN ZERO PRESSURE GRADIENT

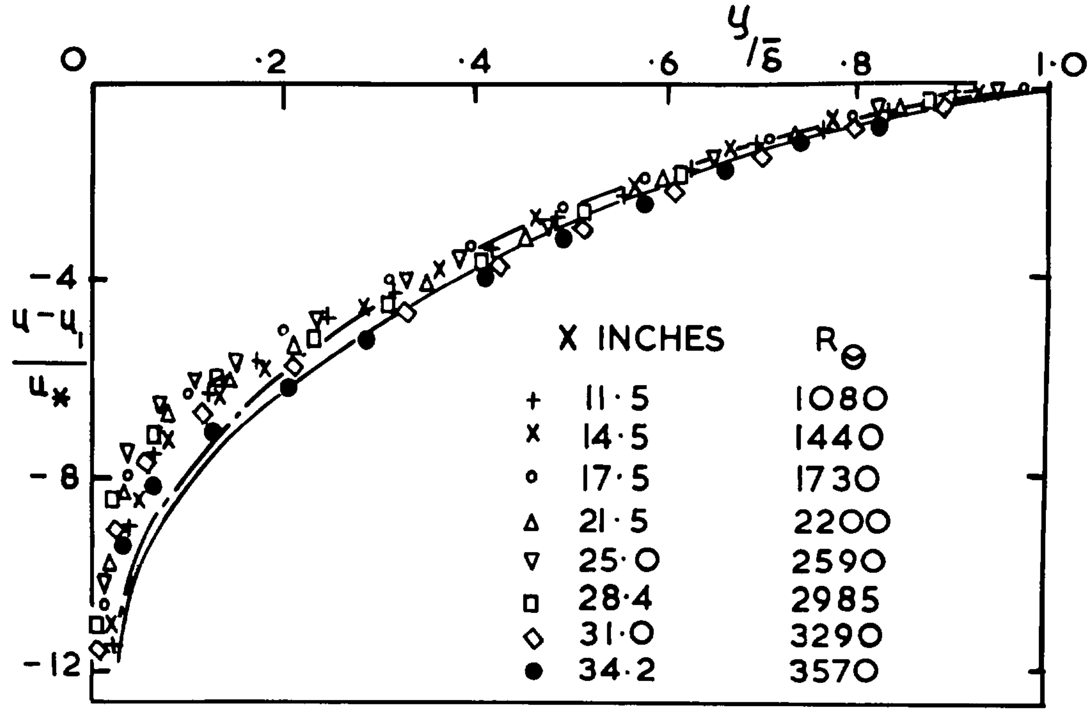

FIG. 9 DATA OF THE AUTHOR: INJECTION IN AN ADVERSE PRESSURE GRADIENT (PRESSURE DISTRIBUTION I)

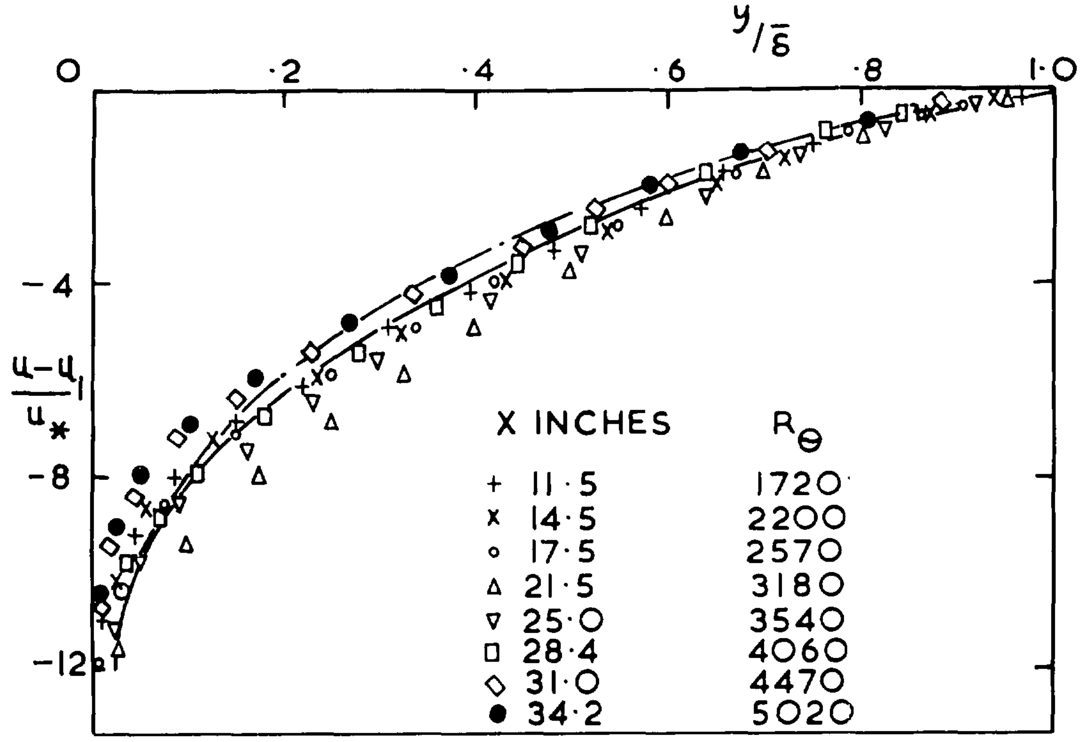

FIG. 10 DATA OF THE AUTHOR: INJECTION IN A FAVOURABLE PRESSURE GRADIENT (PRESSURE DISTRIBUTION II)

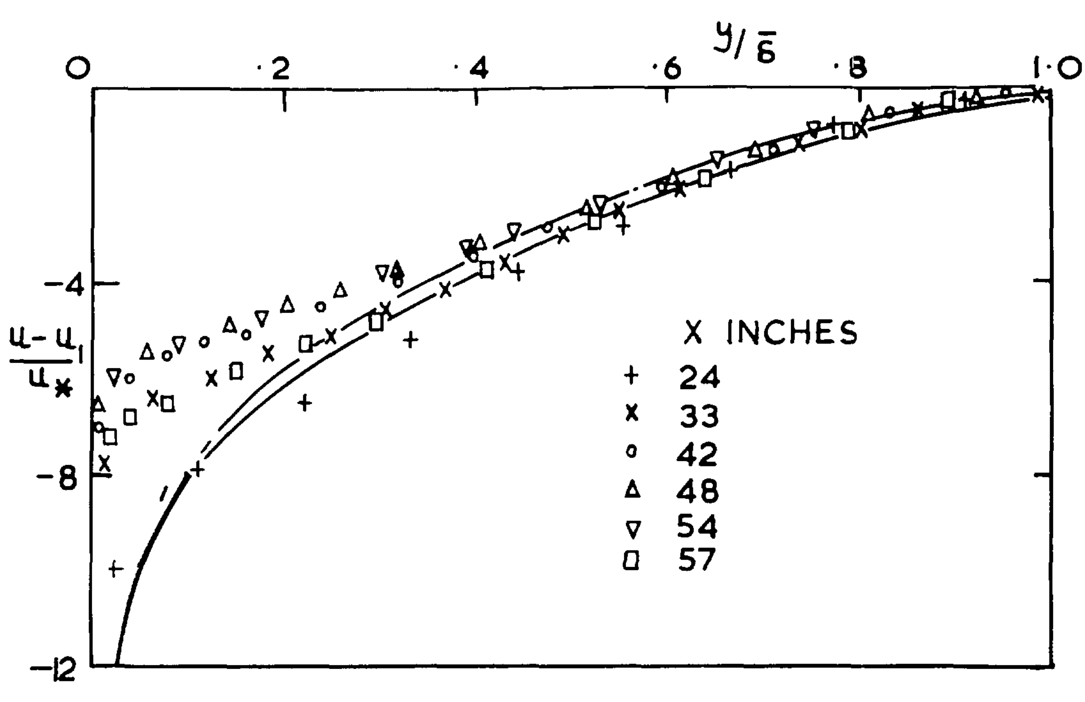

FIG. 11 NEWMAN SERIES II (1951) ADVERSE PRESSURE GRADIENT ON A SOLID SURFACE

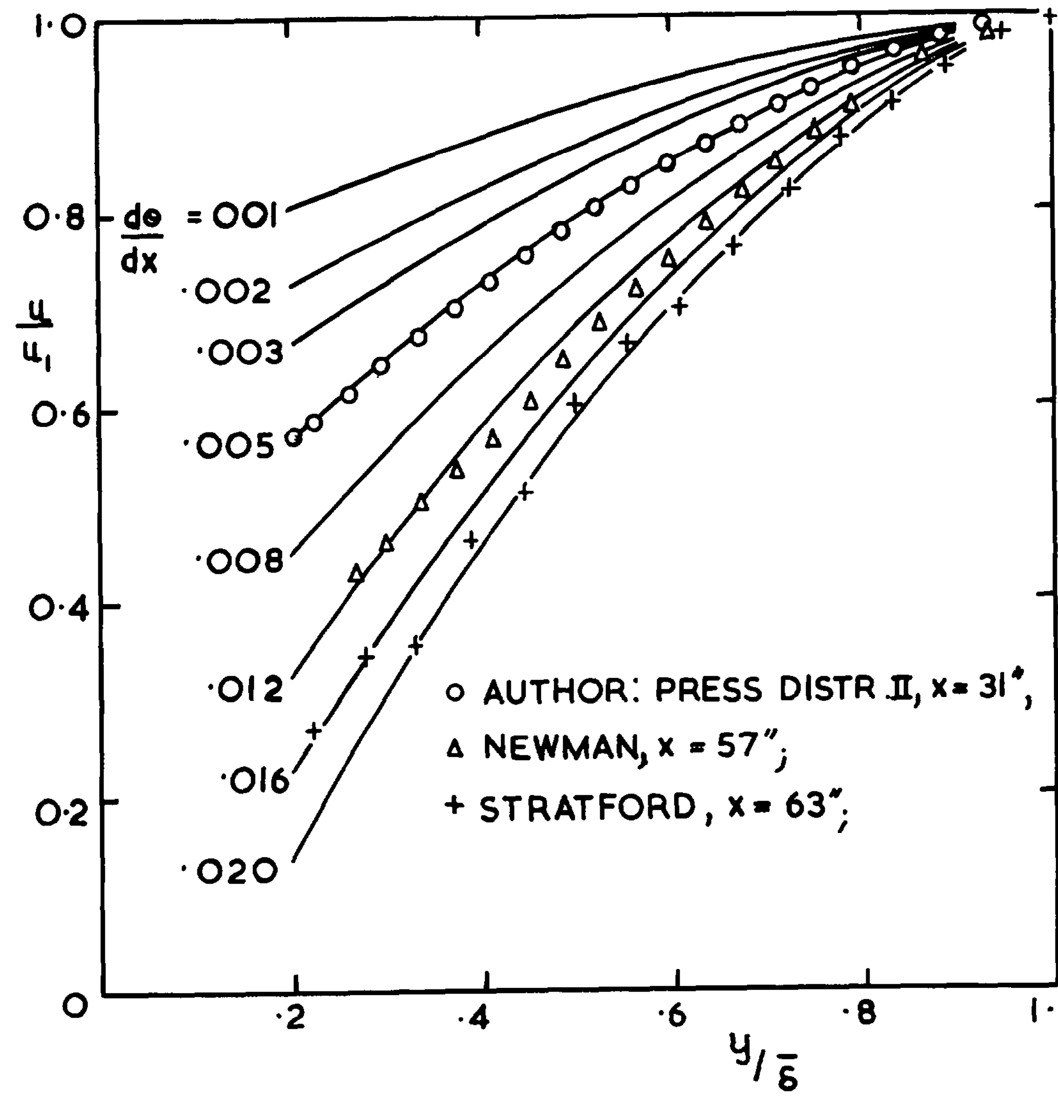

FIG.12 COMPARISON OF EXPERIMENTAL VELOCITY PROFILES WITH VELOCITY DEFECT RELATIONSHIP

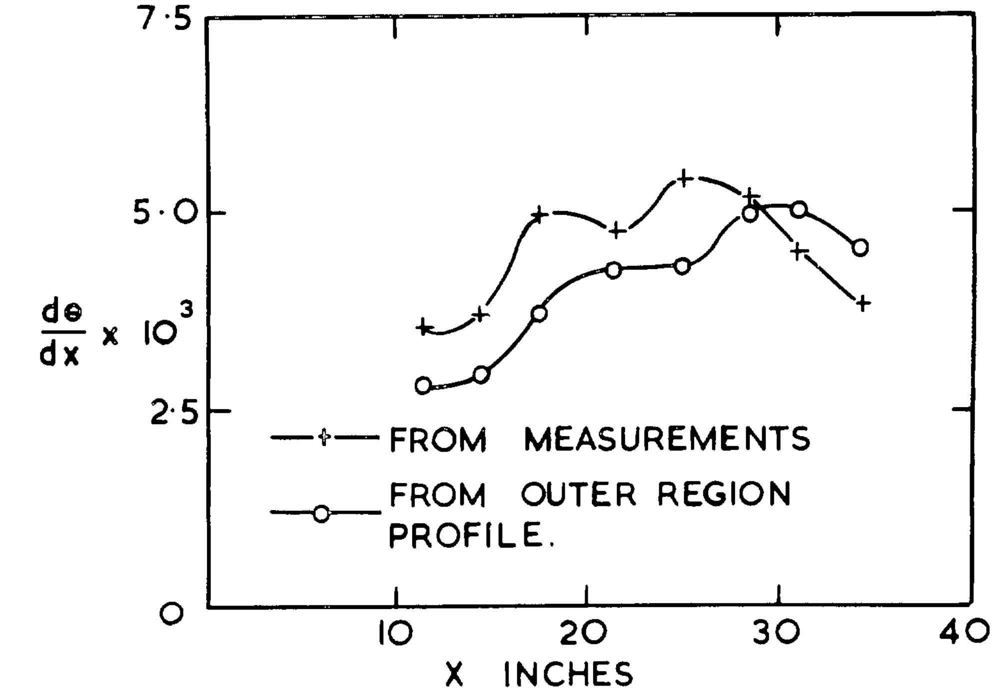

(a) PRESSURE DISTRIBUTION I

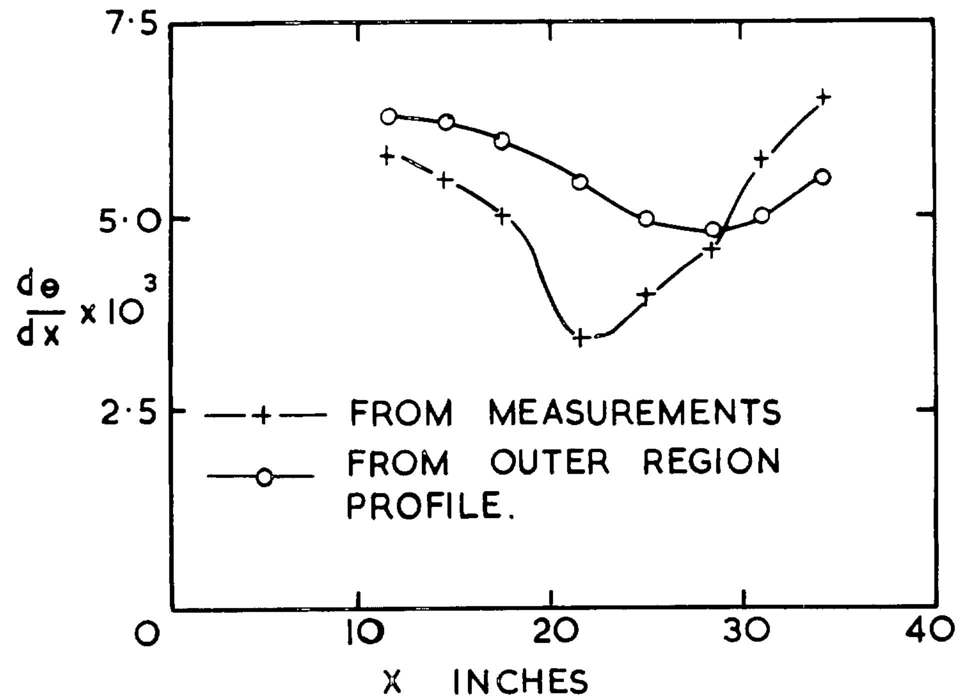

(b) PRESSURE DISTRIBUTION II

FIG. 13 COMPARISONS OF $d\theta/dx$ FROM OUTER REGION PROFILES WITH MEASURED VALUES

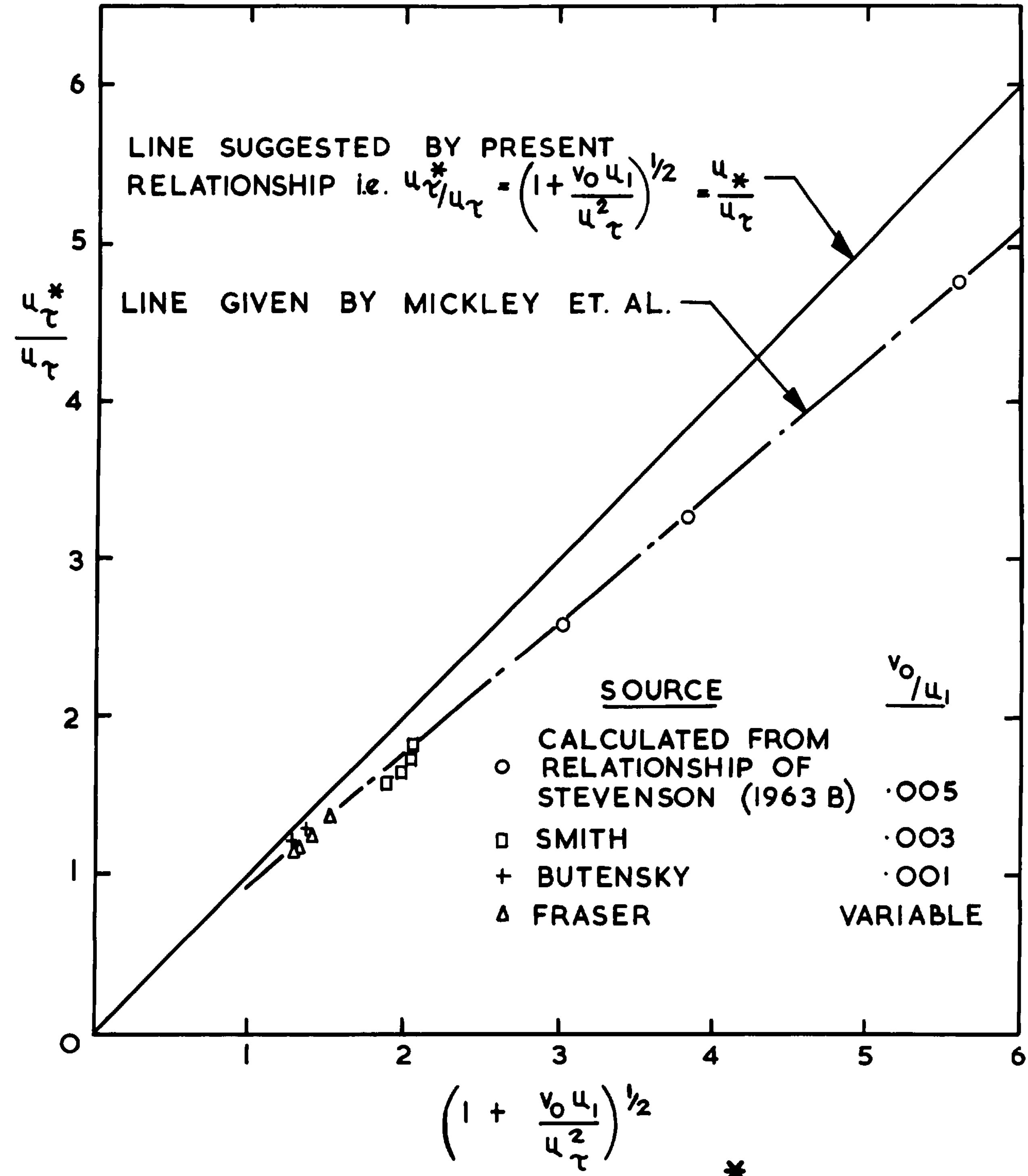

FIG 14 CORRELATION OF u_τ^*/u_τ AGAINST $\left(1 + \frac{v_0 u_1}{u_\tau^2}\right)^{1/2}$ REPRODUCED FROM MICKLEY ET. AL. (1965)

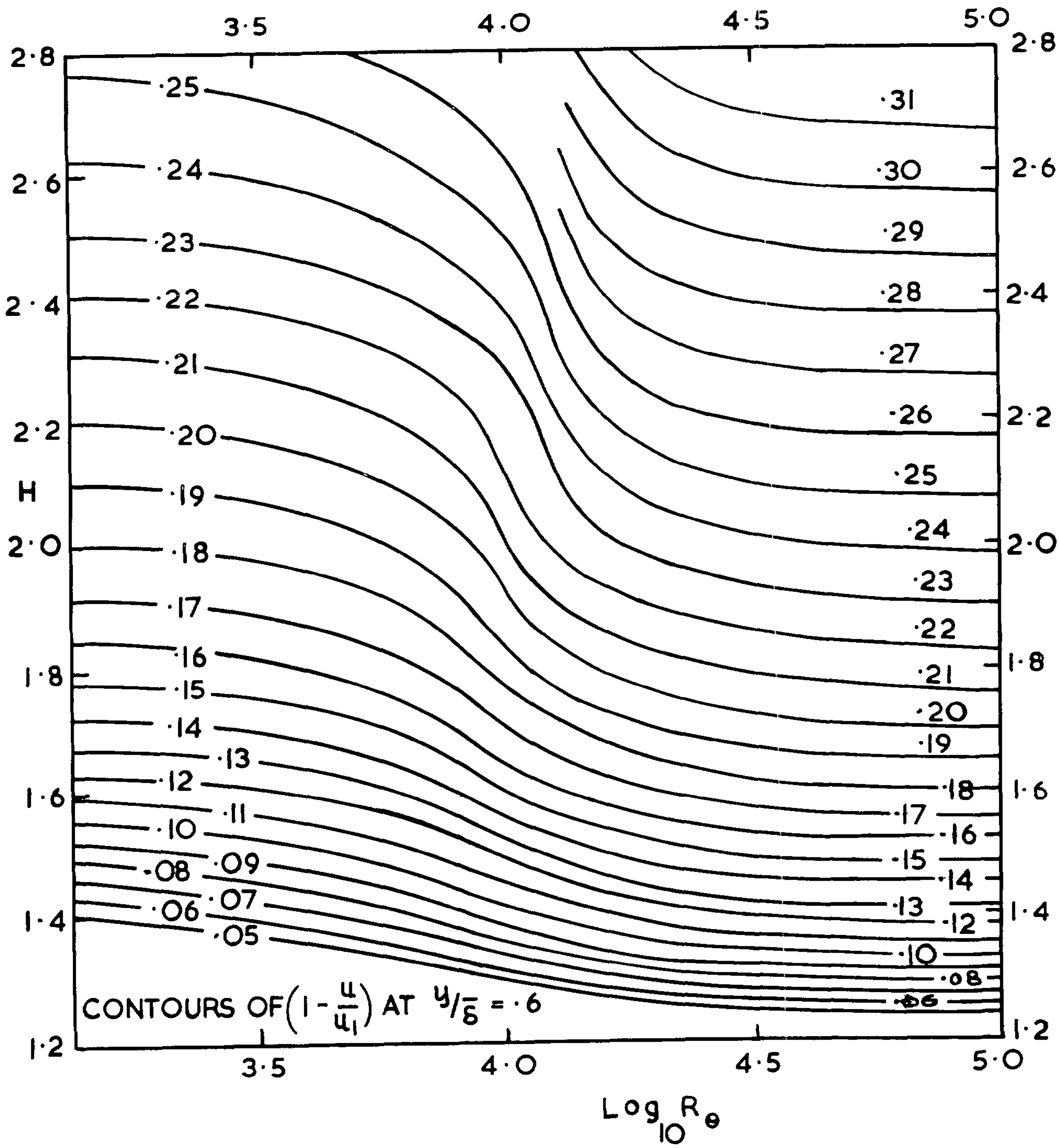

FIG. 15 CHART FOR THE DETERMINATION OF H

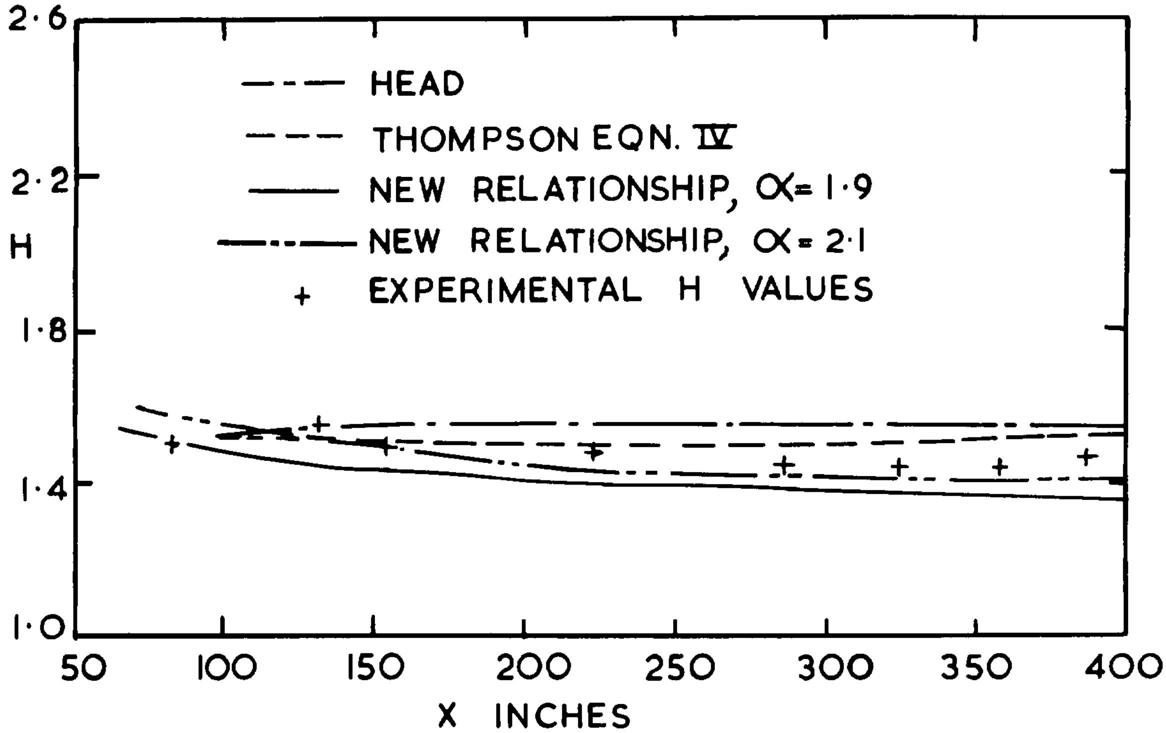

(a) CLAUSER (1954) PRESSURE DISTRIBUTION I

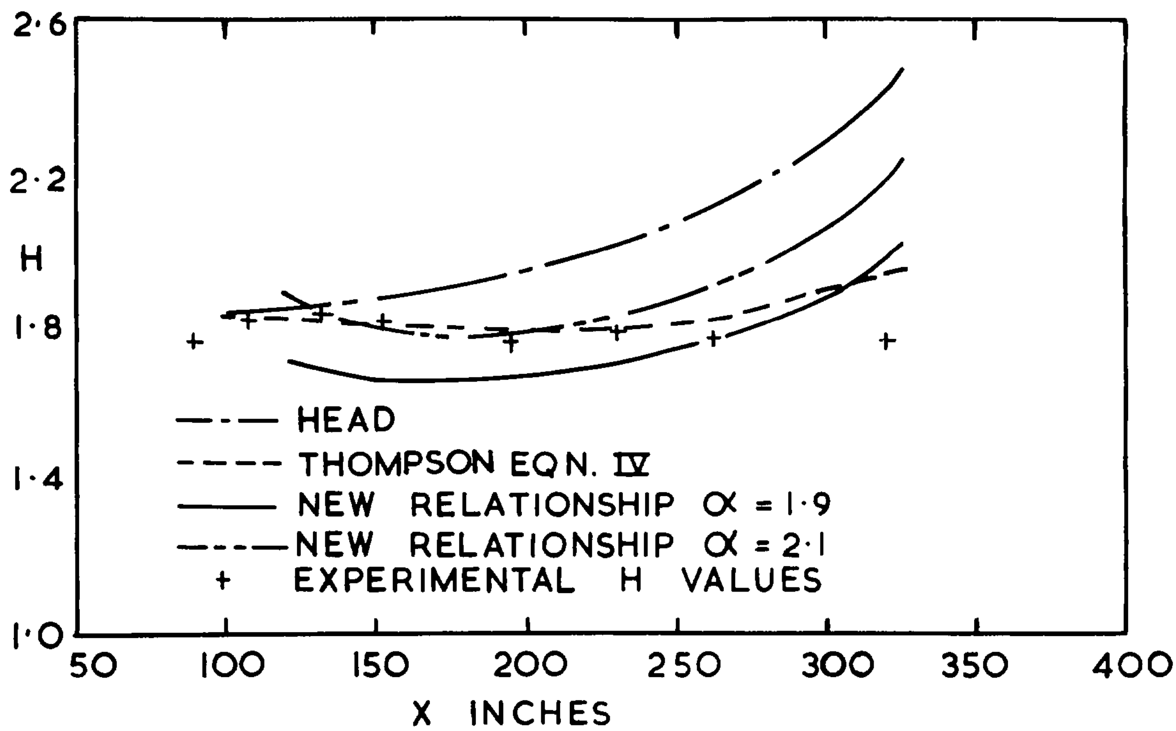

(b) CLAUSER (1954) PRESSURE DISTRIBUTION II

FIG. 16 COMPARISON OF PREDICTED H DEVELOPMENT WITH EXPERIMENT

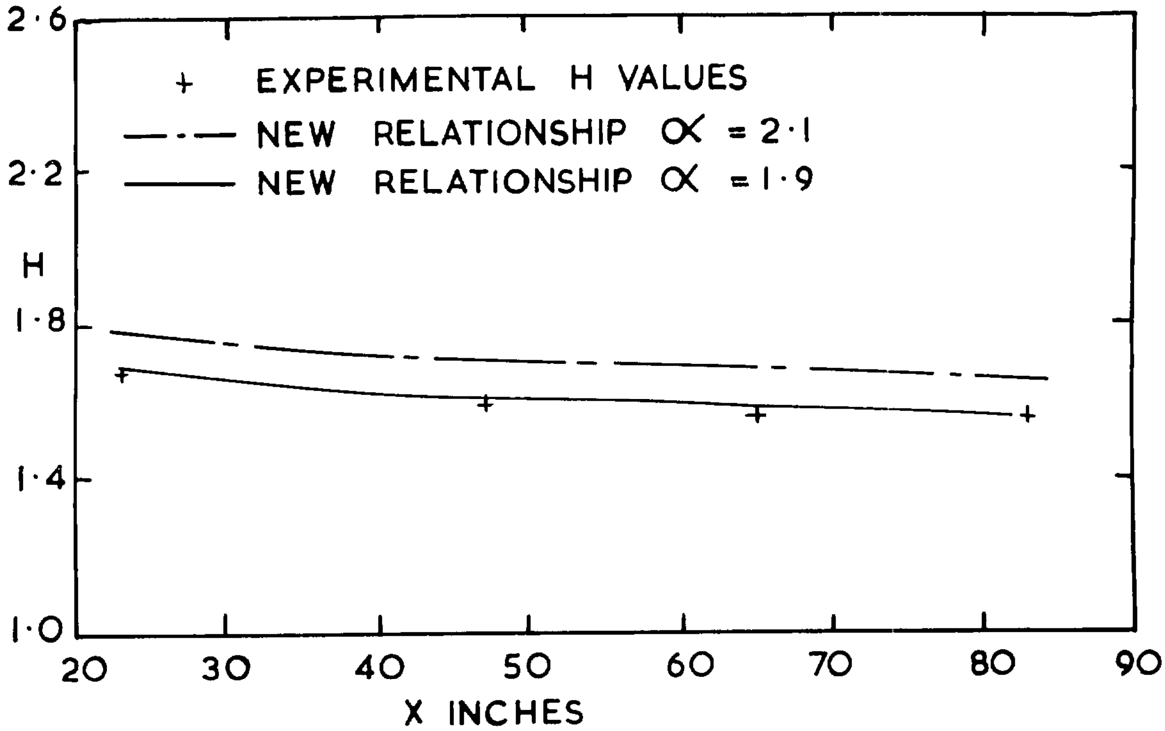

(c) EQUILIBRIUM LAYER OF BRADSHAW (1965)

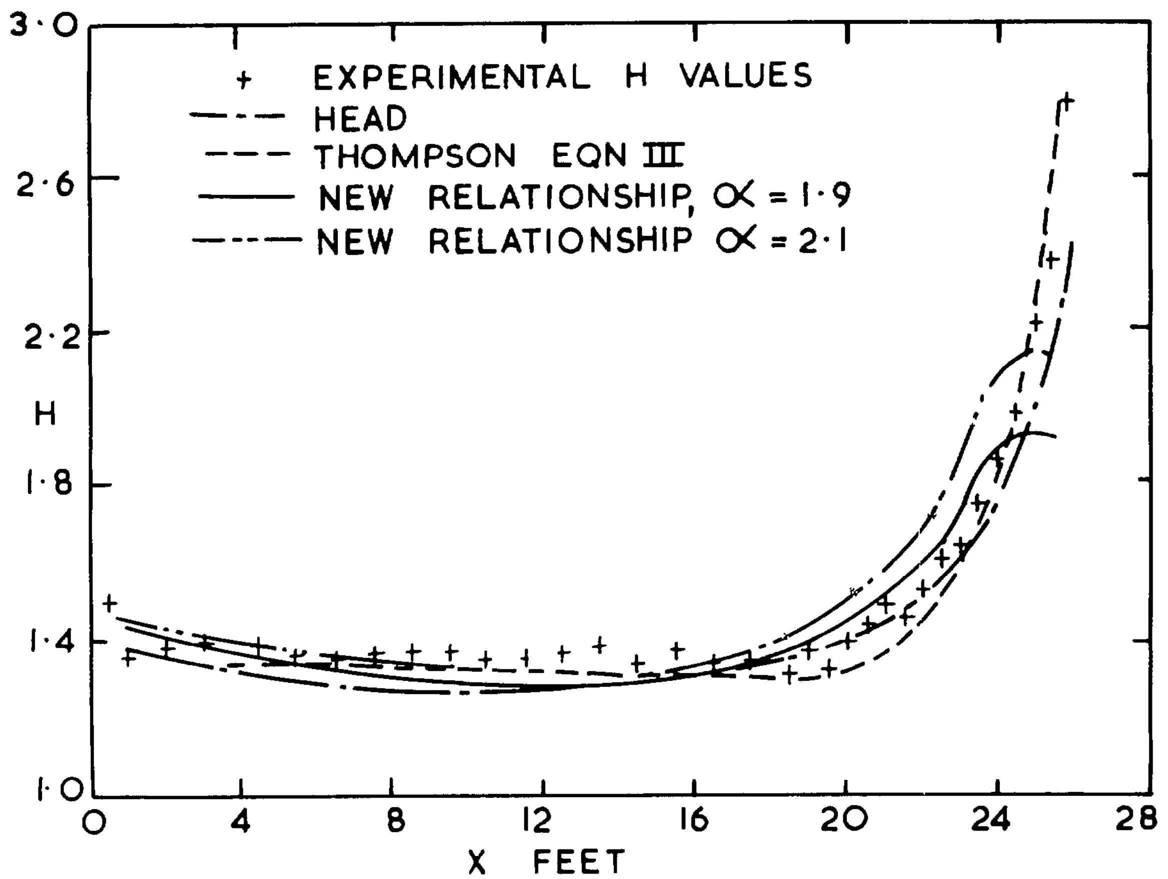

(d) SCHUBAUER AND KLEBANOFF (1951)

FIG. 16 CONT.

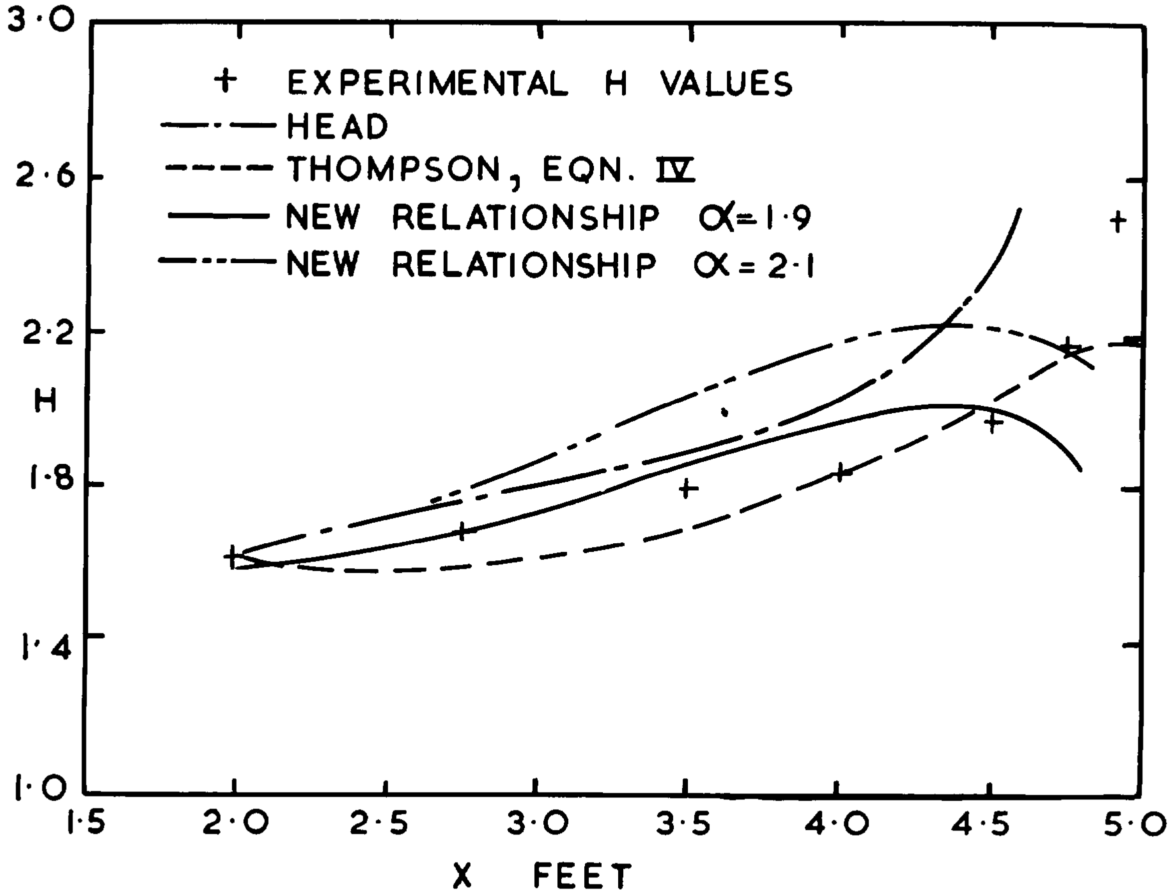

(e) NEWMAN (1951) SERIES II

FIG. 16 CONT.

A.R.C. CP. No.885
October, 1965
J. McQuaid

A VELOCITY DEFECT RELATIONSHIP FOR THE OUTER PART OF EQUILIBRIUM AND NEAR-EQUILIBRIUM TURBULENT BOUNDARY LAYERS

It is shown that the outer part of the velocity defect profiles for equilibrium turbulent boundary layers on solid surfaces can be satisfactorily reduced to an almost universal curve by the use of the velocity scale $U_* = U_1(d\theta/dx)^{\frac{1}{2}}$, with $d\theta/dx$ obtained from the momentum integral equation. The procedure thus uses a single scale for the complete range of the pressure gradient parameter π, whereas previously the use of U_τ as in Clauser's formulation is restricted to cases of finite wall shear stress, with an additional scale, as, for example, Mellor and Gibson's 'pressure' velocity U_p, being necessary to

A.R.C. C.P. No.885
October, 1965
J. McQuaid
A VELOCITY DEFECT RELATIONSHIP FOR THE OUTER PART OF EQUILIBRIUM AND NEAR-EQUILIBRIUM TURBULENT BOUNDARY LAYERS

It is shown that the outer part of the velocity defect profiles for equilibrium turbulent boundary layers on solid surfaces can be satisfactorily reduced to an almost universal curve by the use of the velocity scale $U_* = U_1(d\theta/dx)^{\frac{1}{2}}$, with $d\theta/dx$ obtained from the momentum integral equation. The procedure thus uses a single scale for the complete range of the pressure gradient parameter π, whereas previously the use of U_τ as in Clauser's formulation is restricted to cases of finite wall shear stress, with an additional scale, as, for example, Mellor and Gibson's 'pressure' velocity U_p, being necessary to

A.R.C. C.P. No.885
October, 1965
J. McQuaid
A VELOCITY DEFECT RELATIONSHIP FOR THE OUTER PART OF EQUILIBRIUM AND NEAR-EQUILIBRIUM TURBULENT BOUNDARY LAYERS

It is shown that the outer part of the velocity defect profiles for equilibrium turbulent boundary layers on solid surfaces can be satisfactorily reduced to an almost universal curve by the use of the velocity scale $U_* = U_1(d\theta/dx)^{\frac{1}{2}}$, with $d\theta/dx$ obtained from the momentum integral equation. The procedure thus uses a single scale for the complete range of the pressure gradient parameter π, whereas previously the use of U_τ as in Clauser's formulation is restricted to cases of finite wall shear stress, with an additional scale, as, for example, Mellor and Gibson's 'pressure' velocity U_p, being necessary to

A.R.C. C.P. No.885
October, 1965
J. McQuaid
A VELOCITY DEFECT RELATIONSHIP FOR THE OUTER PART OF EQUILIBRIUM AND NEAR-EQUILIBRIUM TURBULENT BOUNDARY LAYERS

It is shown that the outer part of the velocity defect profiles for equilibrium turbulent boundary layers on solid surfaces can be satisfactorily reduced to an almost universal curve by the use of the velocity scale $U_* = U_1(d\theta/dx)^{\frac{1}{2}}$, with $d\theta/dx$ obtained from the momentum integral equation. The procedure thus uses a single scale for the complete range of the pressure gradient parameter π, whereas previously the use of U_τ as in Clauser's formulation is restricted to cases of finite wall shear stress, with an additional scale, as, for example, Mellor and Gibson's 'pressure' velocity U_p, being necessary to

DETACHABLE ABSTRACT CARDS

treat the zero wall stress layer. The present scale reduces to U_τ as required for the constant pressure layer and is simply related to U_p for the zero wall stress layer. The scale is also found to account well for the outer part of near-equilibrium layers, in particular for the constant pressure layer with uniformly distributed injection. Finally, by combining the relationship with the two-parameter family of mean velocity profiles of Thompson, a simple method is obtained for calculating the variation of the shape-parameter, H.

treat the zero wall stress layer. The present scale reduces to U_τ as required for the constant pressure layer and is simply related to U_p for the zero wall stress layer. The scale is also found to account well for the outer part of near-equilibrium layers, in particular for the constant pressure layer with uniformly distributed injection. Finally, by combining the relationship with the two-parameter family of mean velocity profiles of Thompson, a simple method is obtained for calculating the variation of the shape-parameter, H.

treat the zero wall stress layer. The present scale reduces to U_τ as required for the constant pressure layer and is simply related to U_p for the zero wall stress layer. The scale is also found to account well for the outer part of near-equilibrium layers, in particular for the constant pressure layer with uniformly distributed injection. Finally, by combining the relationship with the two-parameter family of mean velocity profiles of Thompson, a simple method is obtained for calculating the variation of the shape-parameter, H.

treat the zero wall stress layer. The present scale reduces to U_τ as required for the constant pressure layer and is simply related to U_p for the zero wall stress layer. The scale is also found to account well for the outer part of near-equilibrium layers, in particular for the constant pressure layer with uniformly distributed injection. Finally, by combining the relationship with the two-parameter family of mean velocity profiles of Thompson, a simple method is obtained for calculating the variation of the shape-parameter, H.

C.P. No. 885

Printed and published by
HER MAJESTY'S STATIONERY OFFICE
To be purchased from
49 High Holborn, London w.c.1
423 Oxford Street, London w.1
13A Castle Street, Edinburgh 2
109 St. Mary Street, Cardiff
Brazennose Street, Manchester 2
50 Fairfax Street, Bristol 1
35 Smallbrook, Ringway, Birmingham 5
80 Chichester Street, Belfast 1
or through any bookseller

Printed in England

C.P. No. 885

S.O. Code No. 23-9016-85